Geomechanics and Engineering, *Vol. 39, No. 6 (2024) 529-546*
https://doi.org/10.12989/gae.2024.39.6.529

Influence of freeze thaw on stress-strain characteristics and microstructure of cement and fly ash stabilized organic soil

Jiling Zhao[1,2a], Ping Yang*[1], Lin Li[1], Ting Zhang[1] and Haibo Wang[1]

[1]*College of Civil Engineering, Nanjing Forestry University, Nanjing 210037, Jiangsu, China*
[2]*School of Energy Science and Engineering, Henan Polytechnic University, Jiaozuo 454003, China*

(*Received December 1, 2023, Revised December 8, 2024, Accepted December 9, 2024*)

Abstract. Organic soil is often encountered in seasonally frozen areas in China. Before construction, the organic soil is required to be treated to improve its engineering performance due to the high moisture content and low bearing capacity. Cement and fly ash were adopted in this study to treat organic soil subjected to natural freeze-thaw cycles. The influences of freeze-thaw cycles on the stress-strain behavior and microstructure of cement and fly ash-stabilized organic soil (C-F-S-O-S) were evaluated using unconsolidated undrained triaxial (U-U), mercury intrusion porosimetry (MIP) and CT experiments. With and without freeze-thaw cycles, results indicate that the specimen with 20% cement and 5.0% fly ash content performed the best in strength and was selected to evaluate the influence of freeze-thaw cycles on C-F-S-O-S mechanical and microstructure characteristics. The strength, elastic modulus (E-M), cohesion, and internal friction angle of the specimen show the largest decrease of 9.27%, 13.97%, 3.45%, 5.19% after the first freeze-thaw cycle and then slow decreased with further increase of the number of freeze-thaw cycles. The strain corresponding to the peak stress increased with increasing freeze-thaw cycles, and the increase was the largest with a value of 10.19% after the first freeze-thaw cycle. Relationships between the number of freeze-thaw cycles and above parameters were established. A generalized model was also established to predict the stress-strain curve of the C-F-S-O-S. The applicability of the proposed model was validated with published experiment data. The specimen porosity increased first (by 11.03%) and then gradually stabilized after a series of freeze-thaw cycles as revealed by the MIP. Consequently, MIP and CT analysis reveals the soil structural variation since the freeze-thaw cycle is the main reason of the reduction of the specimen strength after the freeze-thaw cycle.

Keywords: freeze thaw cycles; peak strain; peak stress; stabilized organic soil; stress-strain

1. Introduction

Seasonally frozen soil is widely distributed in the northern and weastern regions of China according to Fig. 1 presented in Zhou *et al*. (2000). A large number of infrastructures (e.g., pipelines, highways, and railways) have been built in these regions (Lin *et al*. 2017, Ma *et al*. 2023), with more planned for the future, some of these infrastructures were built on organic soil layers (Shang *et al*. 2016, Nie *et al*. 2013). This organic soil is typically characterized by high rate of water content, and low strength as explained by Hassan *et al*. (2017), especially in seasonal frozen ground areas. As a result, the organic soil is usually unsatisfactory for construction and should be either avoided or treated, as suggested by Hassan *et al*. (2019) and Santagata *et al*. (2008). The mechanical properties of seasonally frozen soil areas are often influenced by more than zero freeze-thaw cycle each year. This freeze-thaw cycle can significantly reduce soil strength and potentially lead to the instability of buildings as stated by Aldaood *et al*. (2014). Therefore, the strength characteristics of soil influenced by freeze-thaw cycles was extensively investigated in the past.

Many scholars have investigated the mechanical properties of soil affected by freeze-thaw cycles (e.g., Steiner *et al*. 2018, Hadi *et al*. 2021, Azadeh *et al*. 2023, Vakili *et al*. 2022). Some of these studies (e.g., Li *et al*. 2022, Liu *et al*. 2021, Jumassultan *et al*. 2021) have investigated the impact of freeze-thaw cycles on the shear strength parameters of soils treated with curing agent. Orakoglu *et al*. (2017) investigated fly ash-lignin fiber stabilized fine-grained soil using undrained triaxial compression test and found that the inclusion of 8% fly ash and 1% lignin fiber can effectively reduce the strength losses after freeze-thaw cycles. Kakroudi *et al*. (2024) investigates the influence of freeze thaw cycles on the static and microstructure properties of nano-silica and basalt fiber treated soil, the results of tests shown that freeze-thaw cycles reduces the cohesion of treated soil and the specimen stabilized with nano-silica has a dese microstructure, enhanced adhesion between soil particles and fibers. Liu *et al*. (2021) investigated the characteristics of cement stabilized silty soil with the impact of freeze-thaw cycles through number of triaxial compression experiments and revealed that the specimens strength increased significantly with increasing cement content before and after freeze-thaw cycles. Similarly, Peng *et al*. (2021) conducted triaxial

*Corresponding author, Professor
E-mail: yangping@njfu.edu.cn
[a]Ph.D.
E-mail: zhaojiling@njfu.edu.cn

ISSN: 2005-307X (Print), 2092-6219 (Online)

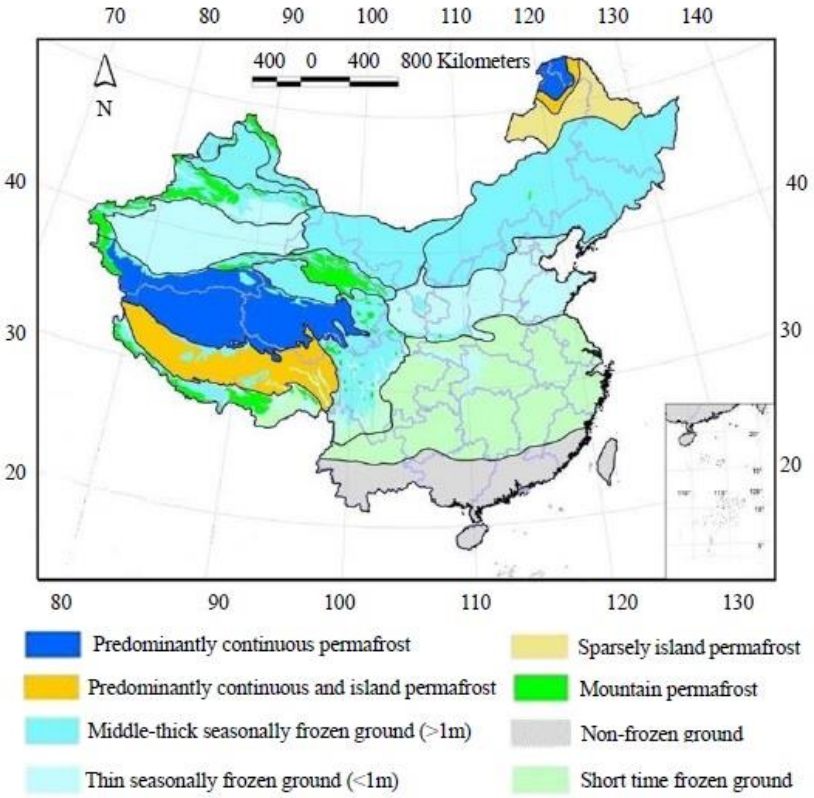

Fig. 1 Distribution of frozen soil in China provided by Zhou *et al*. (2000)

experiments to characterize the mechanical properties of lime and fly ash stabilized soils experienced freeze-thaw cycles and indicated that soil strength increased due to the inclusion of lime and fly ash.

Cement treatment is able to effectively improve the strength of organic soils. A small amount of fly ash can improve soil relative compaction and produce secondary volcanic ash reaction. The combination of cement and fly ash provides an economical-efficient and environmentally friendly solution to stabilize organic soil. Extensive research effort has been conducted on cement and fly ash stabilization organic soils (e.g., Kang *et al*. 2017, Rong 2022, Wong *et al*. 2013), and this method has been proved to has positive effects in treating organic soil in non-permafrost areas (Zulkifley *et al*. 2014). The organic soils in cold regions are subjected to repeated freeze-thaw cycles and the influence of freeze-thaw cycle is significant on the performance of C-F-S-O-S.

However, limited attention has been dedicated to evaluating the influence of freeze-thaw cycles on the mechanical properties of C-F-S-O-S. This paper evaluated the impact of number of freeze-thaw cycles on the stress-strain characteristics and behavior of C-F-S-O-S in seasonal frozen ground areas through laboratory U-U, MIP and CT experiments. To be specific, the specimens were prepared at different cement and fly ash contents.

A environment chamber was adopted to simulate the natural one-dimensional freeze-thaw process. The U-U experiments were then conducted on specimens after different number of freeze-thaw cycles at different cell pressures. The experimental results were analyzed and a new model was established to predict the stress-strain curve of C-F-S-O-S subjected to different number of freeze-thaw cycles. Finally, the mechanism of specimen strength reduction after freeze-thaw cycles was revealed through the structural variation identified through MIP and CT tests. Relationship between macro and meso damage variables of C-F-S-O-S under freeze-thaw cycle will also be established.

2. Test and materials

2.1 Materials

Different organic ingredients exist in organic soils from seasonally frozen ground areas and the content of each ingredients varies significantly with the location. For example, Han *et al*. (2012) conducted borehole sampling on foundation soil in multiple areas such as Dashitou, Hanconggou in Jiangyuan Town, and Huangsongdian, the organic content was between 1.01%~62%, and the moisture content was between 23.8%~419%. Among all the main components of organic soil, fulvic acid has been found to have the greatest barrier effect on cement stabilized organic soil, as reported by Skvortsova *et al*. (2018). To estimate the impact of number of freeze-thaw cycles on the mechanical properties of C-F-S-O-S, artificial organic soil was prepared for tests in this study, and it has been used in other some

Table 1 Basic physical parameters and main chemical composition of silty clay

Soil types	Specific gravity	Moisture content (%)	Liquid limit (%)	Plastic limit (%)	Mass fraction (%)			
					SiO_2	Al_2O_3	Fe_2O_3	K_2O
Silty Clay	2.72	24.23	37.50	21.26	61.36	17.28	8.71	4.69

Table 2 Basic parameters and main chemical composition of cement

Specific area surface (m^2/kg)	Density (g/cm^3)	Initial setting time (min)	Final setting time (min)	Mass fraction (%)				
				SiO_2	CaO	Fe_2O_3	Al_2O_3	MgO
358	3.0	225	304	32.73	30.87	11.38	8.67	6.73

Table 3 Basic parameters and main chemical composition of fly ash

Specific area surface (m^2/kg)	Density (g/cm^3)	Mass fraction (%)					
		SiO_2	Al_2O_3	CaO	Fe_2O_3	K_2O	TiO_2
340	2.4	54.94	34.86	2.63	2.52	1.76	1.25

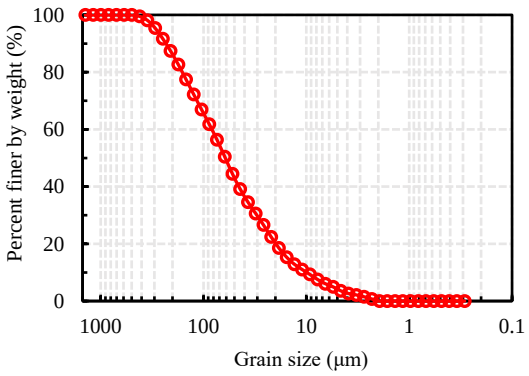

Fig. 2 Grading curve of silty clay

experiments (e.g., Zhong *et al*. 2022, Yunus *et al*. 2015).

Silt with particle size ranging from 0.075~0.002 mm, accounts for approximately 53% and clay with particle size less than 0.002 mm, accounts for about 3% according to the grading curve is shown in Fig. 2. And the basic physical and chemical parameters are shown in Table 1. The cement is PS.A32.5, the chemical composition and basic parameters are shown in Table 2. Fly ash is a first-class high-quality fly ash produced by Yuanxiang Material Factory in Gongyi city, the main chemical composition and basic parameters are shown in Table 3. Fulvic acid ($C_{14}H_{12}O_8$) was purchased from Hefei BASF Biotechnology Co., Ltd. The fulvic acid, dry clay, and water, were mixed to fabricate organic soil (i.e., The density is 1.43 g/cm^3). Portland cement and fly ash were then mixed with the organic soil for specimen preparation. The organic soil was fabricated by adding 10% (i.e., the ratio of the mass of fulvic acid to the mass of the dry soil) fulvic acid and 40% pure water (i.e., the ratio of the weight of pure water to the weight of the dry soil) into oven-dried clay.

2.2 C-F-S-O-S specimen pteparation

It is found that most organic exist in silty clay in seasonally frozen areas of china through extensive literature research (e.g., Wang *et al*. 2023, Wang *et al*. 2022.). The silty clay was oven-dried, pulverized, and then passed a sieve with an opening size of 2.0 mm. The organic soil was made by adding 15% (the ratio of fulvic acid mass to dry soil mass) fulvic acid and 40% water (the ratio of pure water mass to dry soil mass) to the dry soil. Mix the organic soil with water and fulvic acid thoroughly and seal it in a container for at least 24 hours to ensure moisture equilibrium.

Prepare C-F-S-O-S specimens using cement slurry and organic soil. The preparation of these specimens is listed as follows: 1) Weigh a certain amount of cement, fly ash, water, and organic soil; 2) Use a small mixer to thoroughly mix cement and fly ash with water to generate slurry; 3) Add the organic soil to the slurry and continue stir for no less than 10 minutes; 4) Pour the mixture into a mold in three layers; 5) Fix the mold as well as the specimen inside on a vibration platform; 6) Turn on vibration and the vibration duration should be no less than 2 minutes; 7) Trim off excess soil slurry and seal the mold as well as the specimen inside with plastic wrap; 8) Place the mold as well as the specimen inside in an environmental chamber for curing.

Specimens (i.e., height and diameter are 100 mm and 50 mm for U-U testing respectively, height and diameter are 8 mm and 10 mm for MIP testing respectively) were fabricated by compacting the mixture into molds in layers, and the admixture in the mold is placed on a vibration table and compacted for two minutes. The specimens with the mold were stored in an indoor environment for 2 days. After this, the mold was removed and the C-F-S-O-S specimens were kept in a controlled environment at a temperature of 20 ± 3°C for further curing for up to 88 days. The formation and curing of cement soil reference JGJ/T 233-2011 (Specification for mix proportion design of cement soil).

2.3 Curing period of C-F-S-O-S specimen

A certain time is required for the curing before conducting the freeze-thaw cycles. In this test, each specimen experienced 12 freeze-thaw cycles, and one freeze

Table 4 Test conditions

Group	Cement + Fly ash content	Cell pressure (MPa)	freeze-thaw cycles	Curing time (days)
Group I	10% + 5.0%	0.08	0, 1, 3, 6, 12	90
	15% + 5.0%	0.08	0, 1, 3, 6, 12	90
	20% + 5.0%	0.08	0, 1, 3, 6, 12	90
	20% + 0.0%	0.08	0, 1, 3, 6, 12	90
	20% + 2.5%	0.08	0, 1, 3, 6, 12	90
	20% + 7.5%	0.08	0, 1, 3, 6, 12	90
Group II	20% + 5.0%	0.04, 0.08, 0.16	0, 1, 3, 6, 12	90
Group III	20% + 5.0%	0	0, 1, 3, 6, 12	90
Group IV	20% + 5.0%	0	0, 1, 3, 6, 12	90

Note: There are more than 3 cement and fly ash stabilized organic soil specimens were tested for reliable results under each condition

thaw cycle lasting for 24 hours. The effectiveness of cement treatment increases with time, as the cement hydration requires some time. With the progression of hydration, the strength of specimens continues to increase during the freeze-thaw cycle process, which may shade the influence of the freeze-thaw cycles on the reduction of the specimen strength. To minimize this influence, the freeze-thaw cycle should be conducted after the strength of the specimen stabilized with time. According to the existing literature (Lemos *et al*. 2020, Wong *et al*. 2013), C-F-S-O-S strength gradually stabilized after a 90-day curing time. Therefore, this curing time was adopted before conducting the freeze-thaw cycles test in this research.

2.4 Test program

The Standard Test Method for Resistance of Concrete to Rapid Freezing and Thawing (2008) was adopted to simulate the freeze-thaw cycles for the C-F-S-O-S specimens. Note, this freeze-thaw cycle process was conducted without water supply. After the 90-day curing time, immersing the specimens in water more than 48 hours for saturation. To prevent possible soil particles spalling during the freeze-thaw cycles process, filter paper and permeable stones were placed on both ends of the specimen, which were then wrapped with a latex membrane. To reduce moisture loss during the process of freeze-thaw cycles, specimens were wrapped by cling wrap then stored in air-tight bags. Typically, According to Gao *et al*. (2020), Steiner *et al*. (2018), soil strength usually tends to stabilize within the first 10 freeze-thaw cycles. In this study, the maximum number of 12 freeze-thaw cycles was applied. One freeze-thaw cycle was achieved through storing the specimens in an environmental chamber at -20 ºC for 12 hours to achieve frozen and thawing for 12 hours at room temperature. To be specific, the specimens were submerged in water for 48 hours for saturation after the freeze-thaw cycles before conducting the U-U test.

According to Zulkifley *et al*. (2014) and Wong *et al*. (2010) a small amount of fly ash can improve the strength, secondary pozzolanic reaction, and relative compaction of cement stabilize organic soil. With consideration of this, Preliminary experiments were carried out to select cement and fly ash contents for the stabilization of organic soil based on the performance in strength. Table 4 summarizes the three groups of tests (i.e., I, II, and III) conducted in this study. Group I is conducted to investigate the influence of cement and fly ash content on stress-strain characteristic of the specimen under 0.08 MPa cell pressure. Group II is utilized to analyze the shear parameters of specimens experienced to different freeze-thaw cycles under various cell pressures. Group III (i.e., for MIP test) and Group IV (i.e., for CT test) is carried out to assess the influence of freeze-thaw cycles on specimen pore size.

2.5 Triaxial apparatus

The U-U test is performed to investigate the cement and fly ash stabilized organic soil specimens due to its low permeability. After saturation, the U-U experiments were performed with a GDS strain controlled triaxial test apparatus as shown in Fig. 3. The specimens were immersed in water for more than 48 hours before specimen installation for U-U test. A back pressure (i.e., 0.04 MPa) was applied to saturate the specimen and the saturation was considered to be completed when B value of 95% was reached. The U-U test was stopped when an axial strain of 10% was reached. The loading rate was set to be 0.5 mm/min and each test lasted about 20 minutes. The cell pressure for the specimens after various freeze-thaw cycle was set according to Tab. 4. The data acquisition system recorded real-time axial load, cell pressure, and axial displacement.

2.6 MIP test

MIP test was conducted using an AutoProe IV9500 mercury intrusion apparatus (i.e., show as in Fig. 4) with a maximum attainable pressure of 227.5 MPa. This test can be conducted to measure the pore sizes in a soil. This is because the mercury can only enter into specific pores when a certain level of pressure is reached. The pore size (r) can be expressed by the pressure (P) using the Washburn equation proposed by Washburn (1921), as shown in Eq. (1).

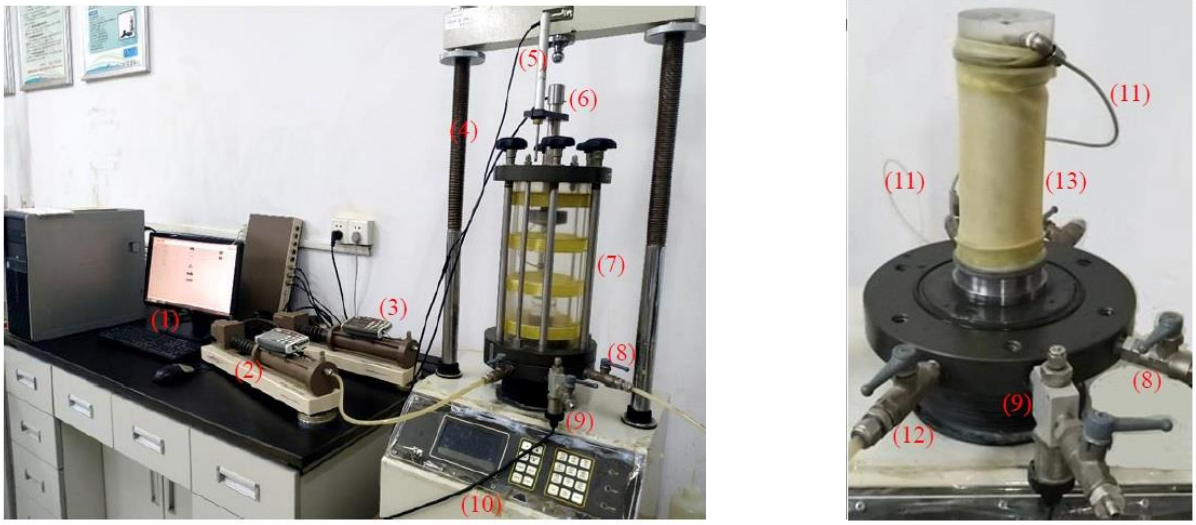

(a) Triaxial device (b) Specimen installation

(1) Data acquisition system, (2) Cell pressure controller, (3) Back pressure controller, (4) Load frame, (5) Displacement sensor, (6) Load cell, (7) Triaxial chamber, (8) Valve for water supply, (9) Pore water pressure sensor, (10) Normal force loading device, (11) Back pressure supply, (12) Cell pressure supply, (13) Latex membrane (thickness of 0.5 mm)

Fig. 3 Static triaxial compression apparatus

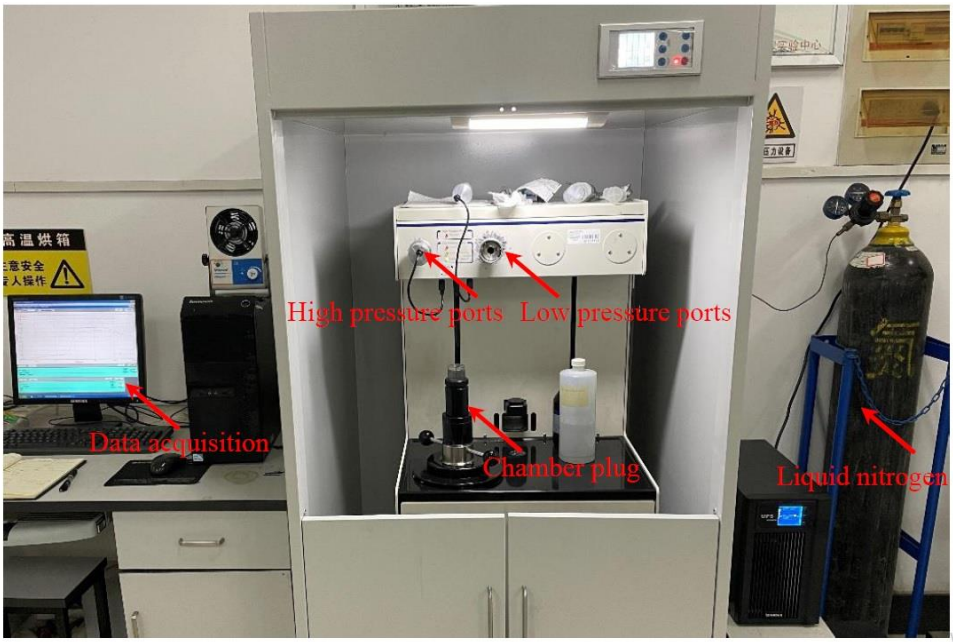

Fig. 4 AutoProe IV9500 mercury intrusion apparatus

$$pr = -2\gamma\cos\theta \quad (1)$$

Where, p is the pressure (MPa), r is the radius of the pores (nm), γ is the Hg surface tension (0.484 N/m) and θ is the contact angle (140.0°).

During the MIP test, mercury first enters the large pores, and as the applied pressure increases, mercury is pushed into the small pores by high pressure. This MIP apparatus is capable of measuring the total pore volume, pore-size, and pore specific area for pore-size ranging from 5 nm to 360,000 nm. Before the MIP test, the C-F-S-O-S specimens were dried using a vacuum drying oven.

2.7 CT test

To achieve an accurate description of the microstructure of samples under freeze-thaw cycles. X-ray micro-CT (NanoVoxel-3502E, Produced by Sanying Precision Instruments Co., Ltd, China). A schematic diagram of the CT experimental machine is shown in Fig. 4. The sample was fixed on the CT stage in the X-ray CT scanner. The CT equipment had a pixel resolution of 500 nm, and its maximum power was 25 W. The maximum current and tube voltage were 1 mA and 190 kV, respectively. The X-ray was generated at 110 kV and 130 μA, and the imaging configuration yielded a voxel size of 18 μm, in this

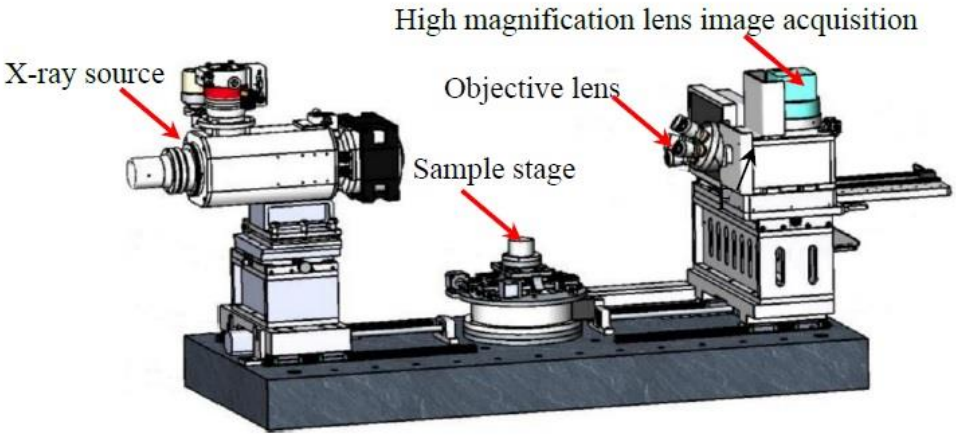

Fig. 5 Schematic diagram of the CT experimental machine

experiment. The internal structure of the CFSOS was tested after being subjected to 0, 1, 3, 6, and 12 freeze-thaw cycles. The samples were scanned at a 0.015 mm interval, 1400 slices were obtained, and a representative five scanning sections of samples were analyzed in this experiment. The dimensions of the gray images were 1000×1000 pixels, and the minimum resolution was 0.1 mm.

3. Results and analysis

3.1 Stress-strain characteristics of the C-F-S-O-S influenced by freeze-thaw cycles

Due to the high strength of stabilized, the increase of its strength only have a small increase with a small changes in cell pressures. According to Wang *et al.* (2023), and Zhang *et al.* (2021), the depth of seasonally frozen soil is usually between 0~4 m, and the corresponding confining stress is approximately 0~0.08 MPa, and vehicle loads will increase the lateral pressure on the subgrade soil according to Tang *et al.* (2020). For measure the shear strength parameters of stabilized soil with different cell pressures under freeze-thaw cycles, a cell pressure of 0.04~0.16 MPa was selected.

To investigate the impact of cement and fly ash content on stress-strain characteristics of organic soil specimens under 0, 1, 3, 6, and 12 freeze-thaw cycles, a series of U-U experiments were performed on specimens under the same chamber pressure of 0.08 MPa. The stress-strain curves of specimens are presented in Fig. 6. Taking Fig. 6(a) as an example, "10%, 5.0%, and F-T 0" stand for 10% cement content, 5.0% fly ash content, and 0 freeze-thaw cycle, respectively. The specimen deformation occurs in the test with an increase in strain, which resulted in a change in stress-strain behavior and eventually led to a decrease in stress as state by Kamruzzaman *et al*. (2009). Additionally, the raw data of stress-strain curves change fluctuations somewhat due to the high rate of data logging.

The stress-strain curves of the C-F-S-O-S specimens can be categorized into three stages. In stage I, a quick increase of the deviator stress was observed as the strain increases at the beginning of testing. In stage II, with progression of axial strain, the stress continuously increased nonlinearly before reaching its peak value. In stage III, stress starts to decrease after reaching the peak value, and then gradually stabilized with increasing axial strain. For specimens with the same cement and fly ash content, the freeze-thaw cycle lead to a downward shift of stress-strain curves. This strain-softening behavior is similar to other stabilized soils (Liu *et al*. 2021, Orakoglu *et al*. 2017).

The peak deviator stress (which is calculated from $\sigma = \sigma_1 - \sigma_3$) is regarded as strength of the specimen. Fig. 6 indicates the strength of all reinforced specimens decreases as freeze-thaw cycles increases. The clinker minerals were produced (e.g., $3CaO{\cdot}2SiO_2{\cdot}3H_2O$, $6CaO{\cdot}Al_2{\cdot}Fe_2O_3{\cdot}12H_2O$, $3Ca(OH)_2$, etc.) during curing of cement stabilized soil, according to Bergado *et al*. (1996), which worked as binder in soil and act as major strength-enhancing compounds. The strength significantly dropped after the first freeze thaw cycle, decreased by 7.16%, 5.35%, 7.84%, 8.96%, 9.39%, 5.12%, respectively, for the specimen with 20%+7.5%, 20%+5.0%, 20%+2.5%, 20%+0.0%, 15%+5.0%, 10%+5.0%, and continuously decreased and then gradually stabilized as freeze-thaw cycles increasing. A slight down in strength is observed when the number of freeze-thaw cycles increase from 6 to 12 for all specimens. This phenomenon is consistent with the findings presented by other scholars (Tang *et al*. 2017, Xu and Wang, 2022) in which that the soil strengthen decreases significantly after the first freeze thaw cycle and stabilizes after several freeze-thaw cycles. The decrease in soil strength after a freeze-thaw process was because of the water-ice phase change in pores weakened the bonding between soil particles. This phenomenon was also explained in Xu *et al.* (2018).

Fig. 7 shows the C-F-S-O-S specimens after different fr eeze-thaw cycles (i.e., with 0.08 MPa confining pressure) at the end of the U-U triaxial test. It can be seen that similar fa ilure planes were identified for all C-F-S-O-S with or with

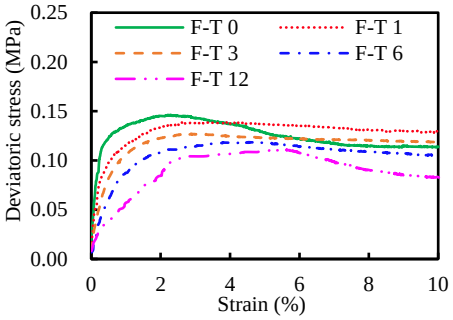

(a) 10%+5.0%

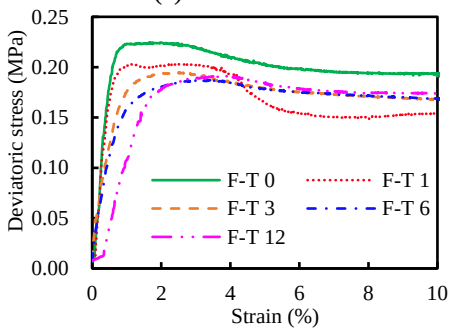

(b) 15%+5.0%

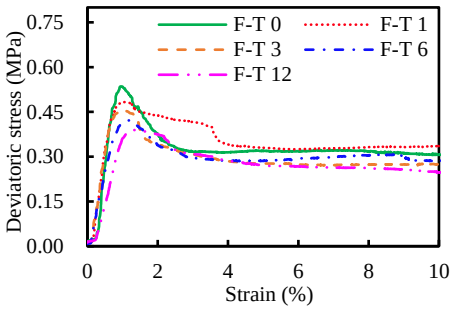

(c) 20%+0.0%

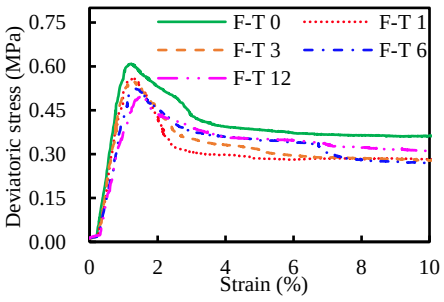

(d) 20%+2.5%

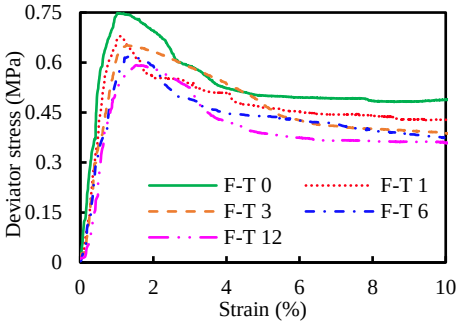

(e) 20%+5.0%

Fig. 6 Stress-strain curves of C-F-S-O-S influenced by various cement and fly ash content under freeze-thaw cycles

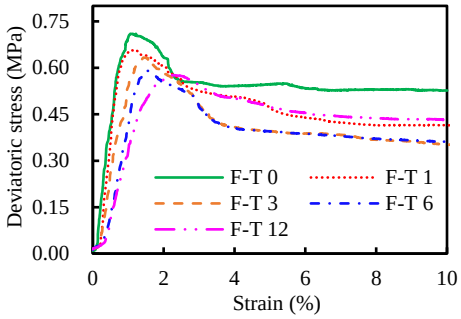

(f) 20%+7.5%

Fig. 6 Continued-

out freeze-thaw cycles. Without a freeze-thaw cycle, no obv ious swelling was observed. After a certain number of freez e-thaw cycles, clear bulging is shown at the middle of the sp ecimen. This is because the freeze-thaw cycles resulted in a deterioration of the soil internal structure and the friction be tween the specimen and the pedestal and loading cap restrai ned the deformation at two ends.

Fig 8 shows the variation of pore water pressure in stabilized organic soil specimens during shearing. Under different confining pressures after different numbers of freeze-thaw cycles, the variations of pore water pressure verses axial strain are similar. To be specific, at the beginning of shearing, a sharp rise in pore water pressure was identified and the peak pore water pressure was usually reached with axial strains less than 2%. With progression of axial strain, excess pore water pressure then gradually dissipated. This is mainly because that part of the axial load applied on the specimen was carried by pore water at the beginning of shearing. With progression of axial strain, more and more axial load was transferred to the soil skeleton which resulted in a decrease in pore water pressure. The effect of freeze-thaw cycles on the variation of pore water pressure during the shearing is not significant. The strain corresponding to the peak pore water pressure increases with increasing number of freeze-thaw cycles

The cement and fly ash has a considerable influence on the strength and freeze-thaw resistance of C-F-S-O-S. Within a cement content of 20%, as shown in Fig. 9, an increase in cement content has a positive effect on improving the strength before and after freeze-thaw cycles. However, with a fly ash content of 5%, when the cement content increased from 10% to 15%, the increase in soil strength was insignificant. To be specific, the soil strength increased by 1.72 times and 5.32 times when the cement content increased from 10% to 15% and 20%, respectively, after 12 freeze-thaw cycles. The improvement in strength is notable when the cement content increased from 15% to 20%. In other words, a threshold content exists when stabilizing organic soils with cement. Comparing with soils without organic, more stabilizer is needed to improve the strength of organic soil.

Small amounts of pozzolanic such as fly ash can be added to cement stabilized organic soil can enhance the secondary pozzolanic reaction, the chemical reaction is as shown in Eq. (2), according to Janz and Johansson (2002).

(a) F-T 0 (b) F-T 1 (c) F-T 3 (d) F-T 6 (e) F-T 12

Fig. 7 Shear failure diagram of C-F-S-O-S affected under different number of freeze-thaw cycles

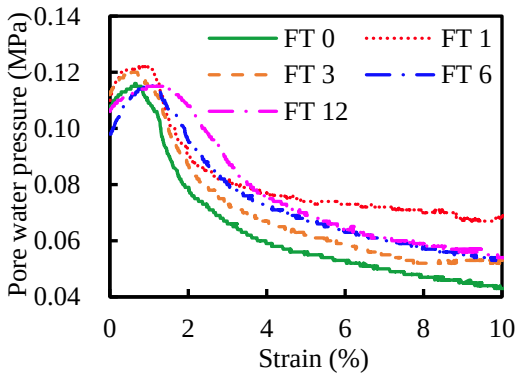

(a) 0.04 Mpa

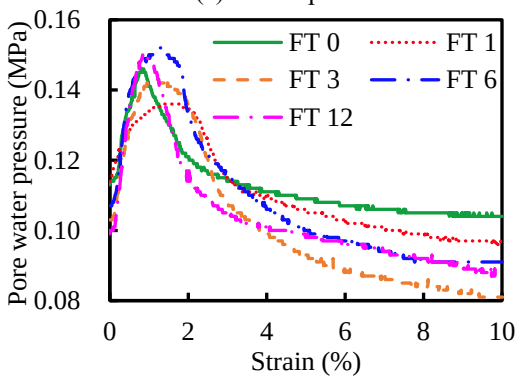

(b) 0.08 Mpa

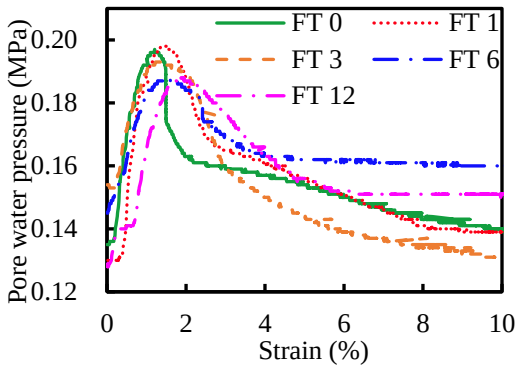

(c) 0.16 Mpa

Fig. 8 Variation of pore water pressure in shear process of C-F-S-O-S under different confining pressures and number of freeze-thaw cycles

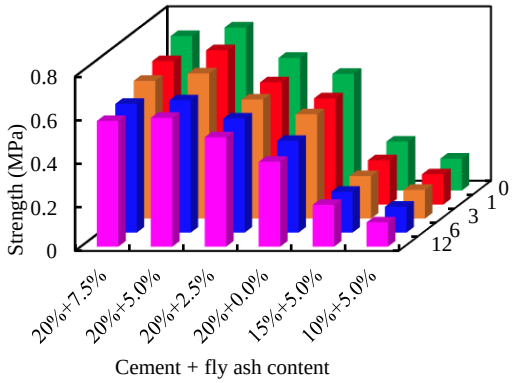

Fig. 9 Cement and fly ash stabilized soil strength variation

As shown in Fig. 9, with the same cement content of 20%, the variation in the specimen strength after the same number of freeze-thaw cycles is significant when there is a change in fly ash content. With freeze-thaw cycle increased from 0 to 12, the strength of the specimens with 0.0%, 2.5%, 5.0% and 7.5% fly ash contents decreased by 27.29%, 17.59%, 20.89% and 18.84%, respectively. At the same cement content of 20%, the strength of the specimen with 5.0% fly ash content is higher than that with 7.5% fly ash. Therefore, it is important to note that an optimal fly ash content exists when cement together with fly ash are used to stabilize soil, this phenomenon may be explained by a condition whereby it has achieved optimal effect of hydration reaction.

$$15Ca(OH)_2 + 10SiO_2 + 25H_2O = 15CaO.10SiO_2 38H_2O \quad (2)$$

U-U compression experiments were conducted to evaluate the variations of the C-F-S-O-S strength after freeze-thaw cycles. Fig. 10 depicts the stress-strain curve of the C-F-S-O-S with 20% cement and 5.0% fly ash content subject to 0, 1, 3, 6, and 12 freeze-thaw cycles under different cell pressures (i.e., 0.04 MPa, 0.08 MPa, and 0.16 MPa). The results demonstrate that an increase in cell pressure results in a corresponding increase in strength before or after freeze-thaw cycle. The strength of C-F-S-O-S before freezing increased by 18.48% and 58.6% with the cell pressure increased from 0.04 to 0.08 and 0.16 MPa, respectively. This was due to the cell pressure increased the

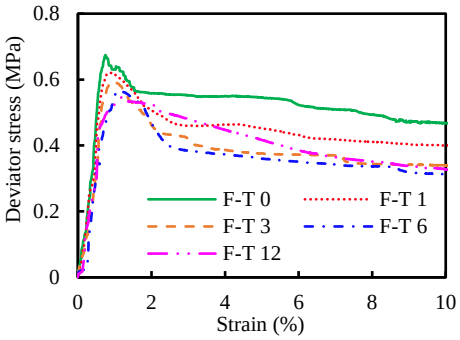

(a) 0.04 Mpa

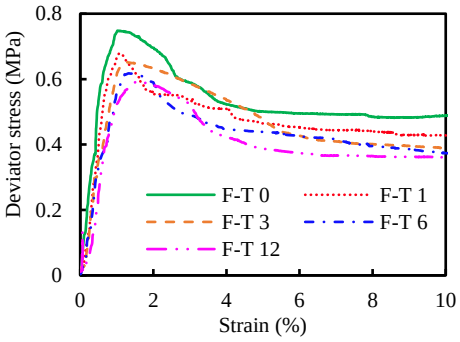

(b) 0.08 Mpa

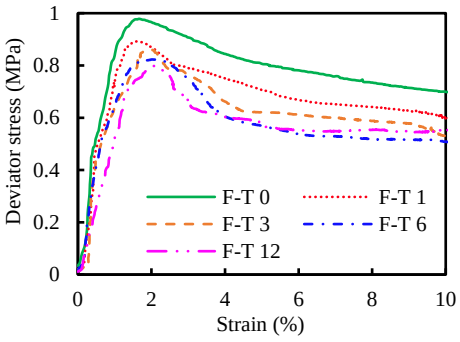

(c) 0.16 Mpa

Fig. 10 Stress-strain curves of specimen with different cell pressures

normal stress on the potential failure plane in the specimen. All cement and fly ash stabilized organic soil specimens exhibited brittle failure under cell pressures within 0.16 MPa.

3.2 Stress-strain model

3.2.1 Peak stress under different cell pressures and freeze-thaw cycles

The Mohr-Coulomb criteria as shown in Eq. (3) is adopted to estimate the influence of freeze-thaw cycles on strength parameters of the C-F-S-O-S specimens.

$$\tau = c + \sigma \tan \varphi \tag{3}$$

Where τ is the shear stress (MPa), σ is the normal stress (MPa), c is the cohesion of soil (MPa), φ is the internal friction angle (º). When the stress reaches its peak value under triaxial loading, the corresponding σ_3 (i.e., the minimum principle stress, which is equivalent to the

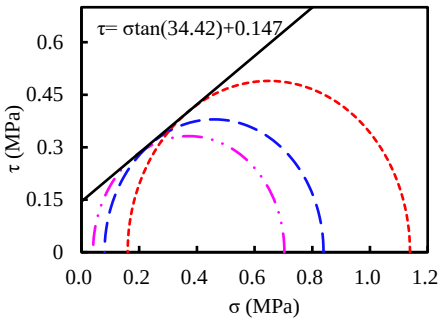

(a) 0 freeze-thaw cycle

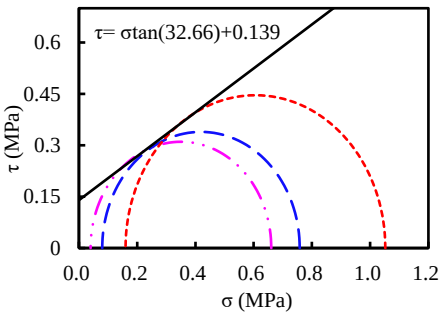

(b) 1 freeze-thaw cycle

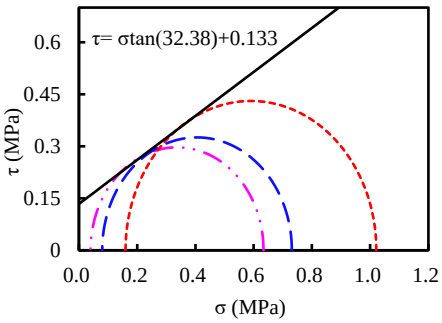

(c) 3 freeze-thaw cycles

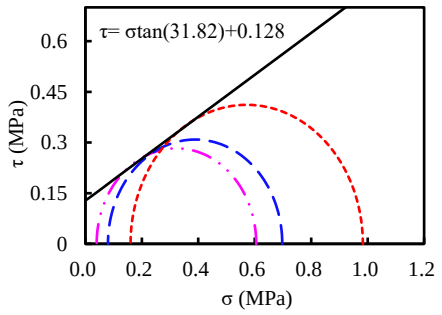

(d) 6 freeze-thaw cycles

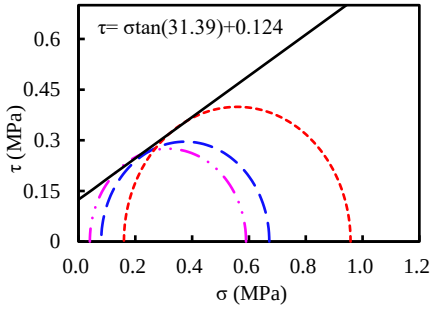

(e) 12 freeze-thaw cycles

Fig. 11 Strength envelopes of the specimen under various freeze-thaw cycles

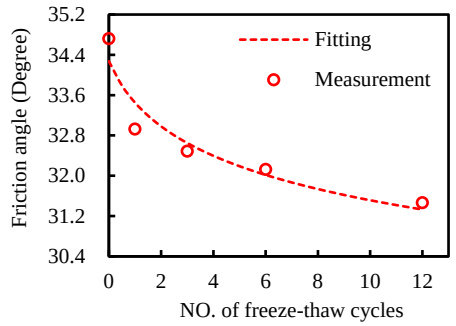

(a) Friction angle

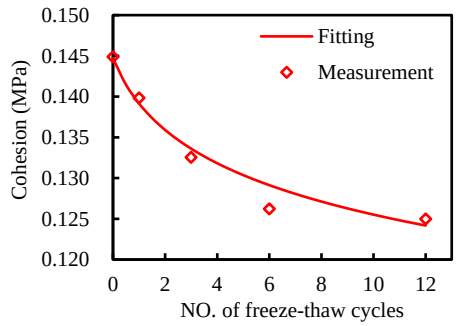

(b) Cohesion

Fig. 12 Correction curves of internal friction angle and cohesion with freeze-thaw cycles

chamber pressure) and σ_1 (i.e., the maximum principle stress, which is the sum of the deviator stress and chamber pressure) could be determined. A Mohr circle can then be plotted on the σ-τ plane with σ_1 and σ_3. Fig. 11 presents the strength envelopes of the C-F-S-O-S with 20% cement and 5.0% fly ash content after different number of freeze-thaw cycles best-estimated according to the Mohr circles through regression. The abscissa of the Mohr circle center is $(\sigma_1 + \sigma_3)/2$ and the ordinate is $(\sigma_1 - \sigma_3)/2$ as shown in Fig. 11. The slope value of the tangent to the Mohr circle is equal to the internal friction angle, (i.e., tanφ = slope of the tangent). The ordinate axis and the tangent line intersect at a point, and the value of the ordinate of this point indicates the cohesion of the specimen.

Fig. 12 shows the variations in cohesion and internal friction angle with freeze-thaw cycles. The cohesion and internal friction angle of the specimens without any freeze-thaw cycles were estimated to be 0.147 MPa and 34.32º, respectively. After the first 6 freeze-thaw cycles, the cohesion and friction angle of the specimen dropped more significantly than the last 6 freeze-thaw cycles. Eventually, the cohesion and internal friction angle of the specimen were 0.124 MPa and 31.39º after 12 freeze-thaw cycles, respectively. This result are consistent with many studies (e.g., Xie *et al*. 2015, Zhang *et al*. 2019) in which the soil cohesion decreases with freeze-thaw cycles increase. It is worth noting that the change in internal friction angle with freeze-thaw cycles is a very small value, less than 3º. Two strength parameters were fitted using Eqs. (4) and (5), respectively.

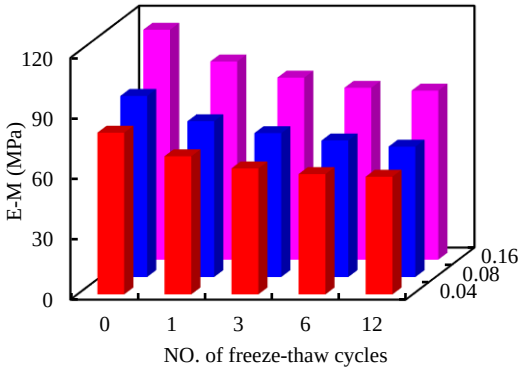

Fig. 13 E-M for C-F-S-O-S specimen with different freeze-thaw cycles

$$\varphi_n = 34.273(n+1)^{-0.035} \tag{4}$$

$$c_n = -0.008\ln(n+1) + 0.1447 \tag{5}$$

($R^2 = 0.9691$, $RMSE = 0.0299$, $MAE = 0.0127$)

Where c_n and φ_n denote the cohesion and friction angle subjected to freeze-thaw cycles, respectively, n is the number of freeze-thaw cycles. Based on the Mohr-Coulomb failure criterion, the peak stress after n freeze-thaw cycles of the specimens can be estimated using Eq. (6) with given number of freeze-thaw cycles and cell pressures.

$$\sigma_{Pn} = \frac{\sigma_3[1+\sin\varphi_n]}{1-\sin\varphi_n} + \frac{2c_n\cos\varphi_n}{1-\sin\varphi_n} \tag{6}$$

Where σ_{pn} is the peak stress after n freeze-thaw cycles of the specimens (MPa), σ_3 is the cell pressure (MPa).

3.2.2 E-M with different cell pressures and number of freeze-thaw cycles

The E-M is a typical parameter widely used in civil engineering. The experimental results of Lee *et al*. (1995) indicate that the stress at 1% strain was a good indicator for describe the five cohesive soils E-M. Liu *et al*. (2016) investigated the E-M of silty sand, taking the stress at 2% strain to calculate the E-M based on the stress-strain curves.

The stress-strain curves (as shown in Fig. 10) indicates that the E-M of a specimen can be calculated by Eq. (7) when the strain is 0.5% (i.e., linear stage).

$$E_n = \frac{\Delta\sigma}{\Delta\varepsilon} = \frac{(\sigma_1-\sigma_3)_{0.5\%} - (\sigma_1-\sigma_3)_{0\%}}{\varepsilon_{0.5\%} - \varepsilon_0} \tag{7}$$

Where E_n is the specimen E-M under n freeze-thaw cycles (MPa), $(\sigma_1 - \sigma_3)_{0.5\%}$ indicates the deviator stress at 0.5% strain (MPa), $(\sigma_1 - \sigma_3)_0$ represents the initial deviator stress (MPa), ε_0 represents the initial strain (%), $\Delta\sigma$ is the increment of deviator stress (MPa), $\Delta\varepsilon$ is the increment of strain (%).

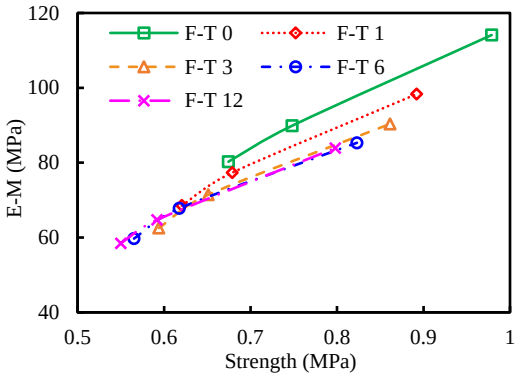

Fig. 14 Relationship between E-M and strength for C-F-S-O-S specimen with different freeze-thaw cycles

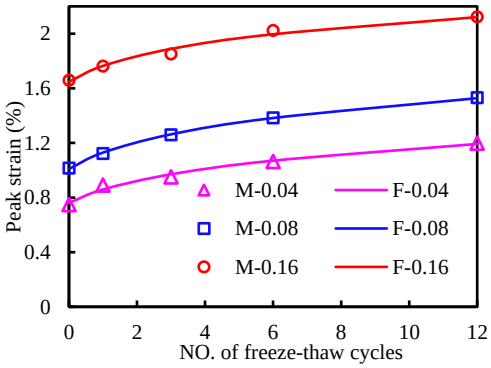

Fig. 15 Peak strain variation of specimens after different freeze-thaw cycles with different cell pressure

Table 5 Regression equation between strength and E-M for the specimens with different freeze-thaw cycles

freeze-thaw cycles	Relation between σ_n and E_n	R^2	*RMSE*	*MAE*
0	$109.75\sigma_{pn}+6.90$	0.998	5.668	5.594
1	$106.63\sigma_{pn}+3.51$	0.993	1.172	1.035
3	$106.02\sigma_{pn}+4.41$	0.987	4.327	4.089
6	$95.35\sigma_{pn}+7.18$	0.986	4.715	4.414
12	$106.02\sigma_{pn}+4.59$	0.994	4.163	4.032

Fig. 13 presents the E-M variations of the tested specimens under different number of freeze-thaw cycles with different cell pressures. Comparing Figs. 13 and 9, it is found that the change trends in the strength and E-M of specimens after freeze-thaw cycles are similar. The specimen E-M decreased as a rise in the number of freeze-thaw cycles, regardless of the cell pressure. The most significant decrease was observed in E-M of the C-F-S-O-S after the first freeze thaw cycles. In addition, the high cell pressure induced a higher specimen E-M, Xu and Wang (2022) also obtained similar conclusions regarding the mechanics of silty clay in their research

For certain types of soil, such as silty sand (Liu *et al*. 2016) and lime-stabilized loess (Zhang *et al*. 2019), a strong link has been observed between strength and E-M after being subjected to different freeze-thaw cycles. The relationship between these two parameters is examined, in this section, and there is a well-defined linear relationship between them is depicted in Fig. 14. As per the observations, there is a linear relationship between strength and E-M. The corresponding regression equation is listed in Tab. 5. Based on Table 5, the relation between strength and E-M can be obtained from Eq. (8).

$$E_n = 104.75\sigma_{Pn} + 5.13 \tag{8}$$

3.2.3 Variation of peak strain with number of freeze-thaw cycles

Fig. 15 shows the change in peak strain of the C-F-S-O-S. The peak strain, defined as strain corresponding to peak stress, increases as freeze-thaw cycles increase. In Fig. 15, taking "M-0.04 and F-0.04" as an example, "M" represents the measurement results, 0.04 represents that the cell pressure is 0.04 MPa, "F" represents fitting results. Eq. (9) presented the correlation between peak strain and number of freeze-thaw cycles. From Table 6, it can be seen that the measured and fitting datasets have a good agreement.

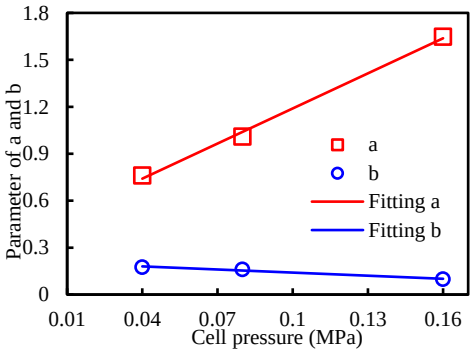

Fig. 16 Variation of parameters *a* and *b* with different cell pressure

Table 6 Regression equation between peak strain and number of freeze-thaw cycles for the specimens with different cell pressures

Cell pressure (MPa)	Relation between ε_{Pn} and freeze-thaw cycles	R^2	*RMSE*	*MAE*
0.04	$0.728(n+1)^{0.256}$	0.954	0.057	0.048
0.08	$1.033(n+1)^{0.1963}$	0.988	0.075	0.060
0.16	$1.618(n+1)^{0.1502}$	0.978	0.039	0.036

$$\varepsilon_{Pn} = a(n+1)^b \tag{9}$$

Where n is the number of freeze-thaw cycles; a and b are two constants dependent on the cell pressure. The relationship between parameters a, b and cell pressure can be expressed by Eqs. (10) and (11), respectively, as shown in Fig. 16.

$$a = 7.474\sigma_3 + 0.442 \tag{10}$$

(R^2=0.996, *RMSE*=0.022, *MAE*=0.020)

$$b = -0.661\sigma_3 + 0.207 \tag{11}$$

(R^2=0.973, *RMSE*=0.006, *MAE*=0.005)

Table 7 Error analysis for prediction of stress-strain of C-F-S-O-S

NO. of freeze-thaw cycles	Cell pressure (MPa)	R^2	RMSE	MAN
0	0.04	0.997	0.023	0.013
	0.08	0.999	0.016	0.010
	0.12	0.994	0.017	0.011
1	0.04	0.999	0.015	0.012
	0.08	0.998	0.030	0.023
	0.12	0.997	0.012	0.007
3	0.04	0.999	0.008	0.005
	0.08	0.996	0.030	0.019
	0.12	0.998	0.028	0.021
6	0.04	0.998	0.014	0.011
	0.08	0.999	0.014	0.010
	0.12	0.989	0.057	0.049
12	0.04	0.997	0.022	0.019
	0.08	0.997	0.023	0.020
	0.12	0.988	0.061	0.055

3.2.4 Normalized stress-strain model of specimen subject to freeze-thaw cycles

Sargin (1971) proposed a stress-strain model for concrete under axial compression, as mathematically shown in Eq. (12). However, the effects of freeze-thaw cycles and cell pressure was not consider in this model.

$$\sigma = \frac{e\frac{\varepsilon}{\varepsilon_p} + (d-1)\times(\frac{\varepsilon}{\varepsilon_p})^2}{1+(e-2)\times(\frac{\varepsilon}{\varepsilon_p}) + d(\frac{\varepsilon}{\varepsilon_p})^2}\sigma_p \tag{12}$$

Where the peak stress and peak strain are denoted as σ_p and ε_p of specimens, respectively. Moreover, e and d are two parameters that control the rising region and the descending region of the stress-strain curve. These parameters can be obtained using Eqs. (13) and (14).

$$e = E\varepsilon_p/\sigma_p \tag{13}$$

$$d = f\sigma_p \tag{14}$$

Where E is the elastic modulus of specimen. f is the empirical coefficient.

Based on Sargin model, a stress-strain model including the peak stress and peak strain of C-F-S-O-S influenced by confining pressures and number of freeze-thaw cycles was established. The model can be modified as follows

$$\sigma_n = \frac{e_1\frac{\varepsilon_n}{\varepsilon_{pn}} + (d_1-1)\times(\frac{\varepsilon_n}{\varepsilon_{pn}})^2}{1+(e_1-2)\times(\frac{\varepsilon_n}{\varepsilon_{pn}}) + d_1(\frac{\varepsilon_n}{\varepsilon_{pn}})^2}\sigma_{pn} \tag{15}$$

Where the peak stress denoted as σ_{pn} (MPa) after n freeze-thaw cycles; the peak strain denoted as ε_{pn} of specimens after n freeze-thaw cycles; e_1 and d_1 can be

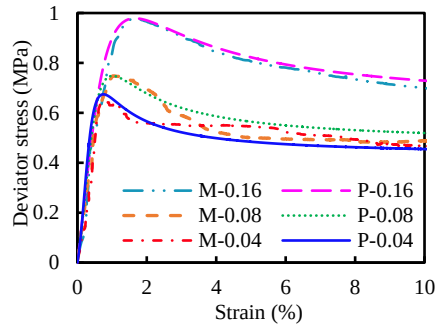

(a) 0 freeze-thaw cycle

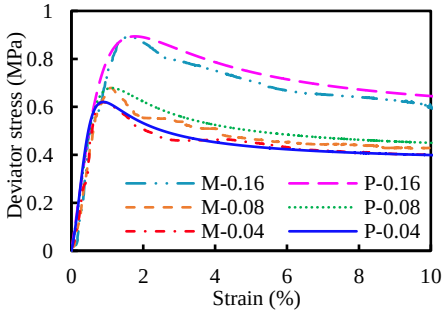

(b) 1 freeze-thaw cycle

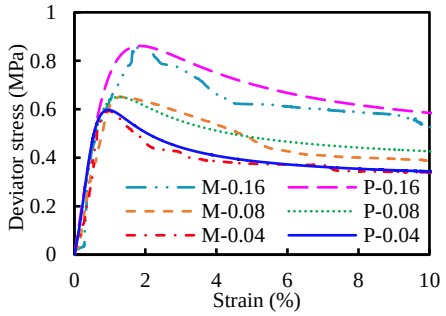

(c) 3 freeze-thaw cycles

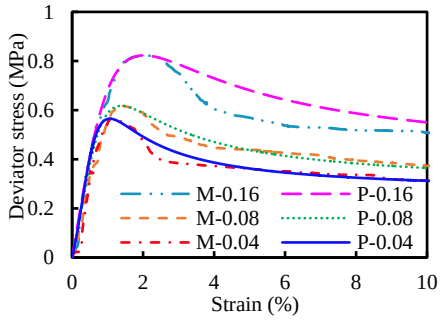

(d) 6 freeze-thaw cycles

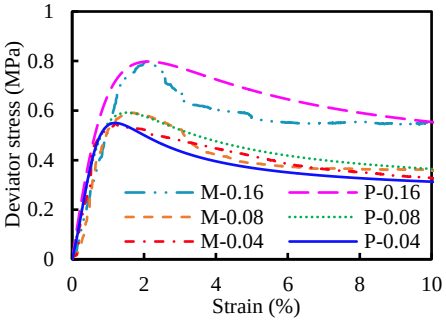

(e) 12 freeze-thaw cycles

Fig. 17 Comparing the measured and predicted results

obtained using Eqs. (16) and (17).

$$e_1 = E_n \varepsilon_{pn} / \sigma_{pn} \tag{16}$$

$$d_1 = g(n+1)^h \tag{17}$$

Where the elastic modulus denoted as E_n (MPa) after n freeze-thaw cycles; g and h is the empirical coefficient, which is 2.652 and -0.157 in this paper.

By combing Eqs. (6), (8), (9), (15), (16) and (17), a normalized stress-strain model of C-F-S-O-S specimen can be obtained to calculate the corresponding stress values with a given strain. The performance of this model was evaluated by comparing the measured and predicted results, as shown in Fig. 17. Taking "M-0.16 and P-0.16" as an example, where 0.16 represents that the cell pressure is 0.16 MPa, "M" represents the measured results, "P" represents the predicted results. The comparison shows that the prediction results by the presented model are in agreement with the measured results of the stress-strain curve.

3.2.5 Verification of stress-strain model

Ai (2023) investigated the static triaxial properties of cement (with a ratio of 2.5%) and clay (with a ratio of 10%) stabilized sand. The stress-strain curves shown strain softening characteristics under different freeze-thaw cycles (0, 1, 4, 7), and the peak stress decreased with the increase of freeze-thaw cycles, while the peak strain increased with the increase of freeze-thaw cycles. To further verify the applicability of the model proposed in this paper, the experimental data of stabilized sand under cell pressure of 0.03 MPa was adopted, and the proposed model parameters are shown in Table 8. The model (19) was used to predict the stress-strain curve of the above soil and compared with the measured data, as shown in Fig. 18, the predicted and measurement results are in good agreement. This indicates that the proposed model in this paper has a wide range of applicability.

3.3 Microstructure analysis

3.3.1 MIP test

After the MIP measurement, the C-F-S-O-S pore size distribution curves can be extracted. Fig. 19 illustrates the influence of freeze-thaw cycle on the structure of C-F-S-O-S with 20% cement and 5.0% fly ash content. The pore size distribution curves of C-F-S-O-S are bimodal. After freeze-thaw cycle, the peaks of pore size distribution curves were significantly increased or shifted to the left compared to the specimens before freeze-thaw cycle. And indicating that freeze-thaw cycles increase the number of small pores. As shown in Fig. 19, the first freeze-thaw cycle resulted in the most significant change of the pore size distribution. However, after several numbers of freeze-thaw cycles, the pore sizes only slightly varied due to further increase of freeze-thaw cycles, since there was no water supplementation (i.e., closed system) during the freeze-thaw cycles process. The variation in the specimen pore size distribution after freeze-thaw cycles are attributed to the water-ice phase change associated volume increase.

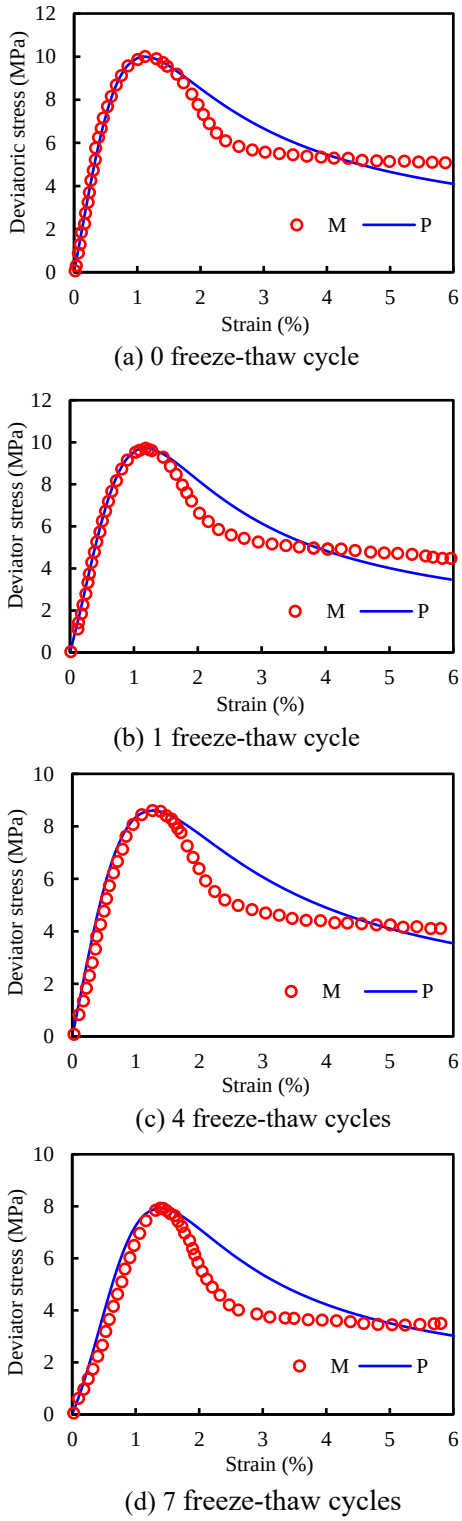

Fig. 18 Comparison of measured and predicted results of cement and clay stabilized sand stress-strain curves under different freeze-thaw cycles

Fig. 20 shows the variation in porosity and strength under cell pressure of 0.04 MPa, 0.08 MPa, 0.16 MPa of the C-F-S-O-S after freeze-thaw cycles. The specimen porosity significant increased by 11.03% after the first freeze thaw cycle. From 1 to 12 freeze-thaw cycles, the porosity only slightly increased with continuous freeze-thaw cycles

Table 8 Model parameters and error analysis of cement and clay stabilized aeolian sand

Number of freeze-thaw cycles	Peak stress (MPa)	Peak strain (%)	Elastic modulus (MPa)	Parameter e_1	Parameter d_1	R^2	RMSE	MAN
0	10.007	1.121	15.494	1.736	1.134	0.9644	0.006	0.003
1	9.723	1.181	12.396	1.505	1.081	0.9674	0.196	0.191
4	8.600	1.264	9.522	1.399	1.068	0.9580	0.006	0.005
7	7.929	1.385	6.049	2.299	0.994	0.9582	0.005	0.005

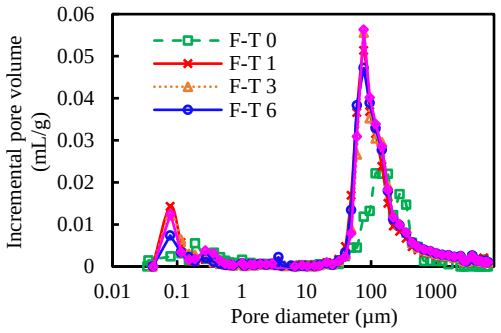

Fig. 19 Pore size distribution of the soil

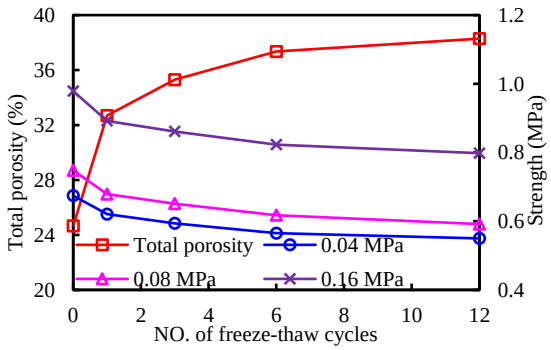

Fig. 20 Porosity and strength change after freeze-thaw cycles

increase. While the soil strength reduced significantly after the first freeze thaw cycle, then gradually stabilized with further increase of freeze-thaw cycles.

According to the damage theory proposed by Kachanov (1992), the defects induce reduction of effective bearing area. To facilitate analysis, the meso damage variable in terms of damage area is defined as follows

$$D_n = 1 - \frac{1-\phi_n}{1-\phi_0} \tag{18}$$

Where D_n is the meso damage variable, ϕ_n is the C-F-S-O-S porosity after n freeze-thaw cycles and ϕ_0 is the C-F-S-O-S initial porosity.

The macroscopic manifestation of damage is the material's mechanical properties deterioration. The deterioration degree can be characterized by the response of macroscopic mechanical properties. Strength can be used to calculating macro damage variable, is defined as follows

$$D_n' = 1 - \frac{\sigma_{pn}}{\sigma_{p_0}} \tag{19}$$

Fig. 21 shows the changes of meso and macro damage variable under freeze-thaw cycle. To be note that the damage variable is 0 of C-F-S-O-S without freeze-thaw cycle. Macro (i.e., 0.04 MPa represents the macro damage variable of the specimen with a 0.04 MPa cell pressure) and micro damage variables of specimens increase as the freeze-thaw cycles increase, and there are small differences in damage evolution pathways. Consequently, the change in specimen microstructure since the freeze-thaw cycle is the main reason for the specimen strength reduction.

Fig. 22 presents the relationship between meso changes and macro mechanical response with the freeze-thaw cycles. The variation of macro damage variables with meso damage variables could be expressed by power function (20), with a fitting degree of over 95%.

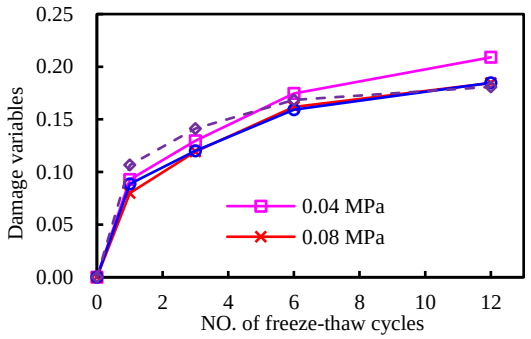

Fig. 21 Macro and meso damage variables evolution with freeze-thaw cycles

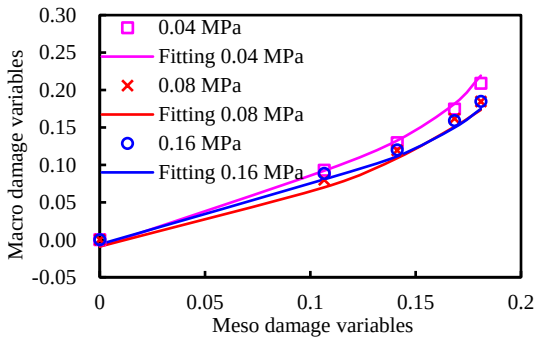

Fig. 22 Relationship between macro and meso damage variables

$$D_n' = jD_n + k \tag{20}$$

Where, j and k are two empirical coefficients related to cell pressure.

Therefore, a stress-strain model considering meso damage with freeze-thaw cycles can be obtained by combining Eqs. (18), (19), (20) and (15), the model can be

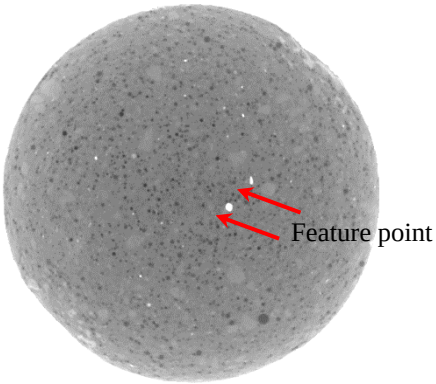

(a) before freezing

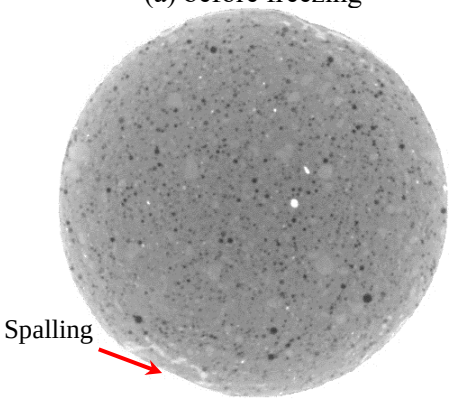

(b) 1 freeze-thaw cycle

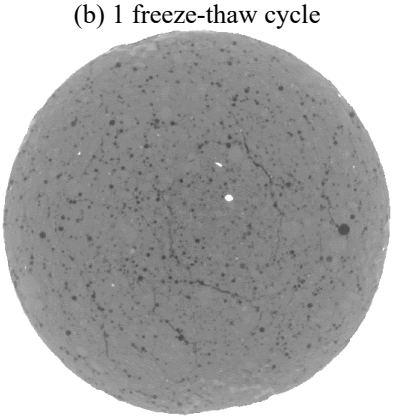

(c) 3 freeze-thaw cycles

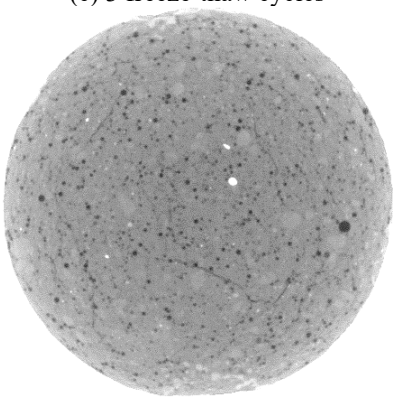

(d) 6 freeze-thaw cycles

Fig. 23 CT scan images of the same section after different number of freeze-thaw cycles

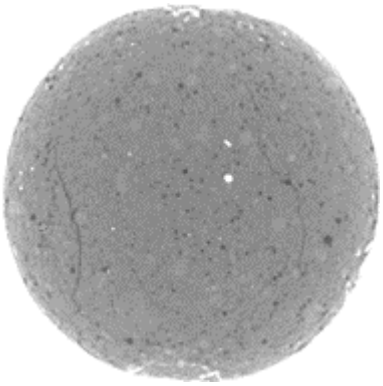

(e) 12 freeze-thaw cycles

Fig. 23 Continued-

written as follows

$$\sigma_n = \frac{e_1 \frac{\varepsilon_n}{\varepsilon_{pn}} + (d_1 - 1) \times (\frac{\varepsilon_n}{\varepsilon_{pn}})^2}{1 + (e_1 - 2) \times (\frac{\varepsilon_n}{\varepsilon_{pn}}) + d_1 (\frac{\varepsilon_n}{\varepsilon_{pn}})^2} [1 - jD_n - k] \sigma_{p0} \quad (21)$$

3.3.2 CT test

The structural variation can provide a better understanding on the deterioration of the cement and fly-ash stabilized organic soils after freeze-thaw cycles. Therefore, in addition to mercury intrusion, CT scanning was also conducted to investigate the structural variation of specimens before and after freeze-thaw cycles. The following Fig. 23 shows the CT image of the cement and fly-ash stabilized organic soil specimen after different number of freeze-thaw cycles. Comparing with the image before the freeze-thaw cycle, spalling was identified at the edge of the specimen after the first the freeze-thaw cycle. After three freeze-thaw cycles, cracks were developed. With continuous increasing number of freeze-thaw cycles, the number and width of the cracks increased.

4. Conclusions

In this study, the stress-strain and microstructure characteristics of the C-F-S-O-S under different number of freeze-thaw cycles were investigated by U-U and MIP tests. While earlier studies have examined the impact of freeze-thaw cycles on stabilized soil, they have not explicitly addressed its influence on stabilized organic soil. The major findings are as follows:

- The inclusion of cement and fly ash improved the strength of the C-F-S-O-S before and after freeze-thaw cycle. The strain-softening behavior of the specimens was observed during the U-U shearing process. In terms of strength, the organic soil with 20% cement and 5.0% fly ash performed the best. After 12 of freeze thaw cycles, the strength of the C-F-S-O-S at this mixing ratio meets the minimum requirements for subgrade soil in the “Technical

Specifications for Construction of Highway Subgrades" (JTG/3610-2019).

- The strength, E-M, cohesion, and internal friction angle of the specimen showing the significant decreased of 9.27%, 13.97%, 3.45%, 5.19% after the first freeze-thaw cycle, and then slow decreased with further increase of the number of freeze-thaw cycles. The strain corresponding to the peak stress increased with freeze-thaw cycles increasing, and the increase was the largest with a value of 10.19% after the first freeze-thaw cycle. Relationships between the above-mentioned parameters and the number of freeze-thaw cycles were also established.
- A model was established to predict the stress-strain curve of the C-F-S-O-S after a certain number of freeze-thaw cycles. The predicted stress-strain curves matched well with the measurement results. And the applicability of the proposed was validated with previous experiment data.
- The MIP and CT experiment results reveal that the C-F-S-O-S structure significantly changed after freeze-thaw cycle. Note that soil porosity increased with freeze-thaw cycles increasing and the influence of the first freeze thaw cycle was the most significant (increased by 11.03%), which explained why soil experienced a significant strength loss after the first freeze-thaw cycle (decreased by 5.35%). And a stress-strain model considering meso damage with freeze-thaw cycles can be obtained.
- The research results of this paper provide a theoretical basis for the influence of freeze-thaw cycles on the mechanical properties of C-F-S-O-S, which is helpful for its application in cold region highway engineering. The influence of different organic contents on the hydration reaction of cement is different. In the future, further research will be conducted on the effect of freeze-thaw cycles on the strength of C-F-S-O-S with different organic contents.

Acknowledgements

The research work herein was supported by the National Natural Science Foundation of China (Grant NO.52178337), the National First-class Disciplines.

References

Ai, H.X. (2023), "Cement-clay improvement of Aeolian sand in seasonally frozen areas research on mechanical properties", Ph.D. Dissertation, Jilin Jianzhu University, Jilin.

Aldaood, A., Bouasker, M. and Al-Mukhtar, M. (2014), "Impact of freeze–thaw cycles on mechanical behaviour of lime stabilized gypseous soils", *Cold Reg. Sci. Technol*., **99**, 38-45. https://doi.org/10.1016/j.coldregions.2013. 1012.1003.

ASTM Standard C666/C666M-603. Standard test method for resistance of concrete to rapid freezing and thawing. ASTM International, 2008.

Bergado, D.T., Anderson, L.R., Miura, N. and Balasubramaniam, A.S. (1996), "Soft ground improvement in lowlands and other environments", 1991st edn. ASCE Press, New York.

Dadfarin, A., Shams Maleki, Y. and Esna-Ashari, M. (2023), "The effects of freeze-thaw cycles on the UCS of 659 the CTS specimens reinforced with DTY fibers", *Constr. Build. Mater*., **393**, 132055. https://doi.org/10.1016/j.conbuildmat. 2023.132055.

Gao, C.H., Du, G.Y., Guo, Q. and Zhuang, Z.X. (2020), "Static and dynamic behaviors of basalt fiber reinforced cement-soil after freeze-thaw cycle", *KSCE J. Civ. Eng*., **24**(12), 3573-3583. https://doi.org/3510.1007/s12205-12020-2266-12205.

Hadi Sahlabadi, S., Bayat, M., Mousivand, M. and Saadat, M. (2021), "Freeze-thaw durability of cement-stabilized soil reinforced with polypropylene/basalt fibers", *J. Mater. Civ. Eng*., **33**(9), 1-14. https://doi.org/10.1061/(ASCE)MT.1943-5533.0003905.

Han, Y.M., Liu, Y. and Che, G.W. (2012), "Research on settlement and deformation characteristics of peat soil roadbed", *Appl. Mech. Mater*., **246-247**, 586-591. https://doi.org/510.4028/www. scientific.net/AMM.4246-4247.4586.

Hassan, N., Wan Hassan, W.H., Rashid, A.S.A., Latifi, N., Mohd Yunus, N.Z., Horpibulsuk, S. and Moayedi, H. (2019), "Microstructural characteristics of organic soils treated with biomass silica stabilizer", *Environ. Earth Sci*., **78**(12), 1-9. https://doi.org/10.1007/s12665-120 19-18369-y.

Hassan, W.H.W., Rashid, A.S.A., Latifi, N., Horpibulsuk, S. and Borhamdin, S. (2017), "Strength and morphological characteristics of organic soil stabilized with magnesium chloride", *Q. J. Eng. Geol. Hydrogeol*., **50**(4), 454-459. https://doi.org/410.1144/qjegh2016-1124.

Janz, M. and Johansson, S.E. (2002), "The function of different binding agents in deep stabilization", Swedish deep stabilization research center, Report No.9, 9–11.

Jumassultan, A., Sagidullina, N., Kim, J., Ku, T. and Moon, S.W. (2021), "Performance of cement-stabilized sand subjected to freeze-thaw cycles", *Geomech. Eng*., **25**(1), 41-48. https://doi.org/10.12989/gae.2021.25.1.041.

Kachanov, M. (1992), "Effective elastic properties of cracked solids: critical review of some basic concepts", *Appl. Mech. Rev*., **45**(8), 304-335. https://doi.org/310.1115/1111.3119761.

Kakroudi, H.A., Bayat, M., Bayat, M. and Nadi, B. (2024), "Static and dynamic characteristics of silty sand treated with nano-silica and basalt fiber subjected to freeze-thaw cycles", *Geomech. Eng*., **37**(1), 85-95. https://doi.org/10.12989/gae.2024.37.1.085.

Kamruzzaman, A.H.M., Chew, S.H. and Lee, F.H. (2009), "Structuration and destructuration behavior of cement-treated singapore marine clay", *J. Geotec. Geoenviron. Eng*., **135**(4), 573-589. https://doi.org/510.1061/(ASCE)1090-0241(2009)1135:1064(1573).

Kang, G.O., Tsuchida, T., Kim, Y.S. and Baek, W.J. (2017), "Influence of humic acid on the strength behavior of cement-treated clay during various curing stages", *J. Mater. Civ. Eng*., **29**(8), 1-18. https://doi.org/10.1061/(ASCE)MT.1943-5533.0001919.

Lee, W., Bohra, N.C., Altschaeffl, A.G. and White, T.D. (1995), "Resilient modulus of cohesive soils and the effect of freeze-thaw", *Can. Geotech. J*., **32**(4), 559-568. https://doi.org/510.1016/0148-9062(1096)83892-83897.

Lemos, S.G.F.P., Almeida, M.S.S., Consoli, N.C., Nascimento, T.Z. and Polido, U. (2020), "Field and laboratory investigation of highly organic clay stabilized with portland cement", *J. Mater. Civ. Eng*., **32**(4), 04020063. https://doi.org/04020010.04021061/(ASCE)MT.040219434025 533.00003111.

Li, K.Q., Liu, Y. and Kang, Q. (2022), "Estimating the thermal conductivity of soils using six machine learning algorithms", *Int. J. Heat Mass Transf*., **136**, 106139.

https://doi.org/106110.101016/j.icheatmasstransfer.102022.106139.

Lin, B., Zhang, F., Feng, D.C., Tang, K.W. and Feng, X. (2017), "Accumulative plastic strain of thawed saturated clay under long-term cyclic loading", *Eng. Geol*., **231**, 230-237. https://doi.org/210.1016/j.enggeo.2017.1009.1028.

Liu, H.B., Sun, S., Wei, H.B. and Li, W.J. (2021), "Effect of freeze-thaw cycles on static properties of cement stabilized subgrade silty soil", *Int. J. Pavement. Eng*., **23**(11), 3770-3782. https://doi.org/3710.1080/10298436.10292021.11919306.

Liu, J.K., Chang, D. and Yu, Q.M. (2016), "Influence of freeze-thaw cycles on mechanical properties of a silty sand", *Eng. Geol*., **210**, 23-32. https://doi.org/10.1016/j.enggeo.2016.1005.1019.

Ma, D.D., Zhang, W.P., Wang, X.P., Zhang, R.R., Zhou, Z.W., Yang, Y. and Shi, Y.H. (2023), "Effects of curing temperature on mechanical properties and pore size distribution of cement clay modified by metakaolin and basalt fiber", *J. Build. Eng*., **68**, 106232. https://doi.org/106210. 101016/j.jobe.102023.106232.

Nie, L., Su, Z.D., Qiao, D.Y. and Yang, X.R. (2013), "Normalized investigation of the peat soil in seasonal frozen region", *Energ. Educ. Sci. Technol. Part A: Energ. Sci. Res.*, **31**(1), 2381-2384.

Orakoglu, M.E., Liu, J.K., Lin, R.B. and Tian, Y.H. (2017), "Performance of clay soil reinforced with fly ash and lignin fiber subjected to freeze-thaw cycles", *J. Cold Reg. Eng*., **31**(4), 04017013.https://doi.org/04017010.04011061/(ASCE)CR.0401 1943-04015495.00000139.

Peng, C., Tian, Z.K., Long, H. and Tan, Y.Q. (2021), "Experiment on the effect of freezing–thawing cyclic on mechanical properties of solidified sludge", *Geotech. Geol. Eng*., **39**(6), 4195-4204. https://doi.org/4110.1007/s10706-10021-1748-10705.

Rong, W. (2022), "Experimental study of strength of cement solidified peat at ultrahigh moisture content", *Geomech. Eng*., **29**(1), 13-23. https://doi.org/ 10.12989/gae.2022.29.1.013.

Santagata, M., Bobet, A., Johnston, C.T. and Hwang, J. (2008), "One-dimensional compression behavior of a soil with high organic matter content", *J. Geotech. Geoenviron. Eng*., **134**(1), 1-13. https://doi.org/10.1061/(ASCE)1090-0241(2008)1134:1061(1061).

Sargin, M. (1971), "Stress-strain relationships for concrete and the analysis of structural concrete sections", Ph.D. Dissertation, University of Waterloo, Ontario.

Shang, W., Wu, X.D., Zhao, L., Yue, G.Y., Zhao, Y.H., Qiao, Y.P. and Li, Y.Q. (2016), "Seasonal variations in labile soil organic matter fractions in permafrost soils with different vegetation types in the central Qinghai–Tibet Plateau", *Catena*., **137**, 670-678. https://doi.org/610.1016 /j.catena.2015.1007.1012.

Skvortsova, E.B., Shein, E.V., Abrosimov, K.N., Romanenko, K.A., Yudina, A.V., Klyueva, V.V., Khaidapova, D.D. and Rogov, V.V. (2018), "The impact of multiple freeze–thaw cycles on the microstructure of aggregates from a soddy-podzolic soil: a microtomographic analysis", *Eurasian Soil Sci*., **51**(2), 190-198. https://doi.org/110.1134/S1064229318020102.

Steiner, A., Vardon, P.J. and Broere, W. (2018), "The influence of freeze–thaw cycles on the shear strength of illite clay", *Proc. Inst. Civ. Eng. Geotech. Eng*., **171**(1), 16-27. https://doi.org/10.1680/jgeen.1616.00101.

Tang, C.X., Lu, Z., Duan, Y.J. and Yao, H. (2020). "Dynamic responses of the pavement-unsaturated poroelastic ground system to a moving traffic load", *Transp. Geotech*, **(25)**:100404.hppts://doi.org/10.1016/j.trgeo.2020.100404.

Tang, L., Tian, S., Ling, X.Z., Li, G.Y. and Zhou, G.Q. (2017), "Effect of freeze-thaw cycles on the strength of base course materials used under China's high-speed railway line", *Cold Reg. Sci. Technol*., **31**(4), 06017003. https://doi.org/06017010.06011061/(ASCE)CR.06011943-06015495.00000125.

Vakili, A.H., Salimi, M., Lu, Y., Shamsi, M. and Nazari, Z. (2022), "Strength and post-freeze-thaw behavior of a marl soil modified by lignosulfonate and polypropylene fiber: An environmentally friendly approach", *Constr. Build. Mater*., **332**, 127364. https://doi.org/10. 1016/j.conbuild mat.2022.127364.

Wang, J.H., Li, Y., Yang, P., Ling, X.Z., Zhao, Y.Y. and Su, L. (2024). "Experimental investigation on dynamic characteristics of fiber-binder modified subgrade filler after freezing-thawing under cyclic loading". *Transp. Geotech*, (39), 100936. hppts://doi.org/1016/j.trgeo.2023. 100936.

Wang, L.X., Song, X.J., Huang, M. and Wang, M. (2022), "Influence factors and prediction method of thermal conductivity for dispersive clay". *J. Hydraul. Eng*., **54**(3), 311-322. https://doi.org/10.13243/j.cnki.slxb. 20220439.

Wang, Y.B., Liu, X., Lv, M.X. and Zhang, Z. (2023), "Mechanisms and influencing factors of hydrothermal processes in active layer soils on the Qinghai-Tibet plateau under freeze-thaw action", *Catena*, **220**(PartA), 106694. https://doi.org/10.1016/j.catena.2022. 106694.

Washburn, E.W. (1921), "Note on a method of determining the distribution of pore sizes in a porous material", *Proc. Natl. Acad. Sci. U. S. A*., **74**(4), 115-116. https://doi.org/110.2307/84084.

Wong, L.S. (2010), "Stabilization of peat by chemical binders and siliceous sand[D]", University of Malaya, Kuala Lumpur (Malaysia).

Wong, L.S., Hashim, R. and Ali, F.H. (2013), "Utilization of sodium bentonite to maximize the filler and pozzolanic effects of stabilized peat", *Eng. Geol*., **152**(1), 56-66. https://doi.org/10.1016/j.enggeo.2012.1010.1019.

Xie, S.B., Quan, J.J., Lai, Y.M., Zhou, Z.W. and Xu, X.T. (2015), "Effects of freeze-thaw cycles on soil mechanical and physical properties in the Qinghai-Tibet Plateau", *J. Mate. Sci*., **12**(4), 999-1009. https://doi.org/1010.1007/s1162911014-13384-11627.

Xu, J., Wang, Z., Ren, J. and Yuan, J. (2018), "Mechanism of shear strength deterioration of loess during freeze-thaw cycling", *Geomech. Eng*., **14**(4), 307-314. https//:doi.org/10.12989/gae.2018.14.4.307.

Xu, W.B. and Wang, X.C. (2022), "Effect of freeze–thaw cycles on mechanical strength and microstructure of silty clay in the Qinghai–Tibet plateau", *J. Cold Reg. Eng*., **36**, 1-11. https://doi.org/10.1061/(ASCE)CR.1943-5495.0000267.

Yunus, N.Z.M., Wanatowski, D., Hassan, N.A. and Marto, A. (2015), "Shear strength and compressibility behaviour of lime-treated organic clay", *KSCE J. Civ. Eng*., **20**(5), 1721-1727. https://doi.org/1710.1007/s12205-12015-10438-12205.

Zhang, Y.Z., Wang, T.L., Kou, X.K., Feng, Z.X. and Liu, W.L., (2021), "Liquid water-vapour migration tracing and characteristics of unsaturated coarse-grained soil in high-speed railway subjected to freezing and different load types", *Constr. Build. Mater*., (283), 122747. hppts://doi.org/10.1016/j.conbuildmat.2021.122747.

Zhong, Y.Q., Cai, G.H., Wang, S.Q., Qin, H,J., Zhang, C.H. and Li, J.S. (2022), "Influence of organic content on the mechanical properties of organic-rich soils stabilized with CaO-GGBS binder and PC mechanical properties of stabilized artificial organic soil", *Water*., **14**(19), 3053. https://doi.org/10.3390/w14193053.

Zhou, Y., Guo, D. and Qiu, G. (2000), "Geocryological regionalization and classification map of the frozen soil in China (1:10,000,000)", A Big Earth Data Platform for Three Poles. https://doi.org/10.11888/Geocry. tpdc.270037.

Zulkifley, M.T.M., Ng, T.F., Raj, J.K., Hashim, R., Bakar, A.F.A., Paramanthan, S. and Ashraf, M.A. (2013), "A review of the stabilization of tropical lowland peats". *Bull. Eng. Geol.*

Environ., **73**(3), 733-746. https://doi.org/10.1007/s10064-013-0549-5.

Zulkifley, M.T.M., Ng, T.F., Raj, J.K., Hashim, R., Bakar, A.F.A., Paramanthan, S. and Ashraf, M.A. (2014), "A review of the stabilization of tropical lowland peats", *Bull. Eng. Geol. Environ.*, **73**(3), 733-746. https://doi.org/710.1007/s10064-10013-10549-10065.

CC